Article

Identification of Thiazolo[5,4-*b*]pyridine Derivatives as c-KIT Inhibitors for Overcoming Imatinib Resistance

Yunju Nam [1,2,3,†], Chan Kim [2,†], Junghee Han [1,2,3], SeongShick Ryu [1,2,3], Hanna Cho [2], Chiman Song [3], Nam Doo Kim [4], Namkyoung Kim [1,2,3] and Taebo Sim [1,2,3,*]

[1] KU-KIST Graduate School of Converging Science and Technology, Korea University, 145 Anam-ro, Seongbuk-gu, Seoul 02841, Republic of Korea
[2] Severance Biomedical Science Institute, Graduate School of Medical Science, Yonsei University College of Medicine, 50 Yonsei-ro, Seodaemun-gu, Seoul 03722, Republic of Korea
[3] Chemical Kinomics Research Center, Korea Institute of Science and Technology, 5 Hwarangro 14-gil, Seongbuk-gu, Seoul 02792, Republic of Korea
[4] Voronoibio Inc., 32 Songdogwahak-ro, Yeonsu-gu, Incheon 21984, Republic of Korea
*   Correspondence: tbsim@yuhs.ac
†   These authors contributed equally to this work.

Simple Summary: c-KIT has been regarded as a promising therapeutic target against gastrointestinal stromal tumor (GIST). Overcoming drug resistance of c-KIT inhibitors including imatinib is required. We designed and synthesized novel thiazolo[5,4-*b*]pyridine derivatives and performed structure-activity relationship (SAR) studies to overcome imatinib resistance. The SAR studies led to the identification of the derivative **6r** as a potent c-KIT inhibitor. The derivative **6r** is capable of strongly inhibiting a c-KIT V560G/D816V double mutant that is resistant to imatinib and remarkably attenuates proliferation of GIST-T1 and HMC1.2 cancer cells. Moreover, **6r** possesses differential cytotoxicity on c-KIT D816V Ba/F3 cells relative to parental Ba/F3 cells. Kinase panel profiling revealed that **6r** has reasonable kinase selectivity. Furthermore, **6r** not only blocks migration and invasion, but also suppresses anchorage-independent growth of GIST-T1 cells.

Abstract: c-KIT is a promising therapeutic target against gastrointestinal stromal tumor (GIST). In order to identify novel c-KIT inhibitors capable of overcoming imatinib resistance, we synthesized 31 novel thiazolo[5,4-*b*]pyridine derivatives and performed SAR studies. We observed that, among these substances, **6r** is capable of inhibiting significantly c-KIT and suppressing substantially proliferation of GIST-T1 cancer cells. It is of note that **6r** is potent against a c-KIT V560G/D816V double mutant resistant to imatinib. Compared with sunitinib, **6r** possesses higher differential cytotoxicity on c-KIT D816V Ba/F3 cells relative to parental Ba/F3 cells. In addition, kinase panel profiling reveals that **6r** has reasonable kinase selectivity. It was found that **6r** remarkably attenuates proliferation of cancer cells via blockade of c-KIT downstream signaling, and induction of apoptosis and cell cycle arrest. Furthermore, **6r** notably suppresses migration and invasion, as well as anchorage-independent growth of GIST-T1 cells. This study provides useful SAR information for the design of novel c-KIT inhibitors overcoming imatinib-resistance.

Keywords: c-KIT; GIST; GIST-T1; HMC1.2; imatinib resistance; thiazolo[5,4-*b*]pyridine

1. Introduction

c-KIT, a class III receptor tyrosine kinase, consists of five immunoglobulin-like domains, one transmembrane domain, one juxta-membrane domain, and two split kinase domains [1]. Binding of a stem cell factor (SCF) ligand to c-KIT induces the c-KIT dimerization, leading to subsequent activation of its intracellular signaling cascades [2]. Dysfunctions of c-KIT, such as gain of function caused by overexpression and point mutation, result in c-KIT activation and tumorigenesis [3,4]. Activation of c-KIT is observed in various cancers

including GIST, mast cell tumors, and malignant melanomas [4–6]. In particular, c-KIT activation is deeply associated with GISTs which are the most common gastrointestinal tumor [7,8]. More than 90% of 419 GIST cases are associated with c-KIT activation and 6−7% of the cases are implicated with PDGFRα mutations [9].

Mutations within exon 11 encoding the juxta-membrane domain of c-KIT, with a relative frequency of 67%, are most common in GIST [10]. The mutations in exon 9 (IgG-like D5 domain of c-KIT) of which the majority are duplications of A502_Y503 occur at nearly 15% in GIST [11,12]. Notably, secondary c-KIT mutations causing imatinib resistance have been known to occur most commonly in exon 13/14 (ATP-binding domain of c-KIT) and exon 17/18 (activation loop of c-KIT) [13–15]. The c-KIT T670I gatekeeper mutant within exon 13 corresponds to the BCR-ABL T315I gatekeeper mutant and causes drug resistance through constitutive activation and steric hindrance [16,17]. D816H/V mutants occurring in the activation loop of c-KIT are capable of accelerating auto-activation rather than wild-type c-KIT, which leads to resistant to imatinib [18]. Moreover, the double mutant of c-KIT V560G/D816V has disruption of auto-inhibitory mechanism and SCF-independent constitutive activation of c-KIT [19].

Imatinib, an innovative BCR-ABL kinase inhibitor against chronic myelogenous leukemia, has been approved as a first-line treatment for advanced GIST (Figure 1) [20]. However, 10–20% of patients taking imatinib show secondary mutations that decrease c-KIT sensitivity to imatinib [21]. Sunitinib, a second-line therapy for the treatment of GIST, possesses inhibitory activity against c-KIT V654A and gatekeeper mutant c-KIT T670I [13]. However, preclinical studies have revealed that both imatinib and sunitinib do not effectively inhibit exon 17 *KIT* mutations (activation loop mutants) [14]. Rego-rafenib was approved for the third-line treatment against imatinib-and sunitinib-resistant GISTs but it has moderate activities against the secondary mutations [22,23]. The potent c-KIT/PDGFRα inhibitor avapritinib has been approved for the GIST treatment [24]. How-ever, secondary PDGFRα mutations (Val658Ala, Asn659Lys, Tyr676Cys, and Gly680Arg) have been observed in patients with drug resistant recurrent GIST [25]. Ripretinib, the fourth-line treatment approved for GIST, interacts reversibly to both the switch pocket and activation loop of c-KIT [26]. Although ripretinib is capable of inhibiting a wide range of c-KIT and PDGFRα mutants, it shows an overall response rate of 9.4%, suggesting additional resistance and disease progression [27].
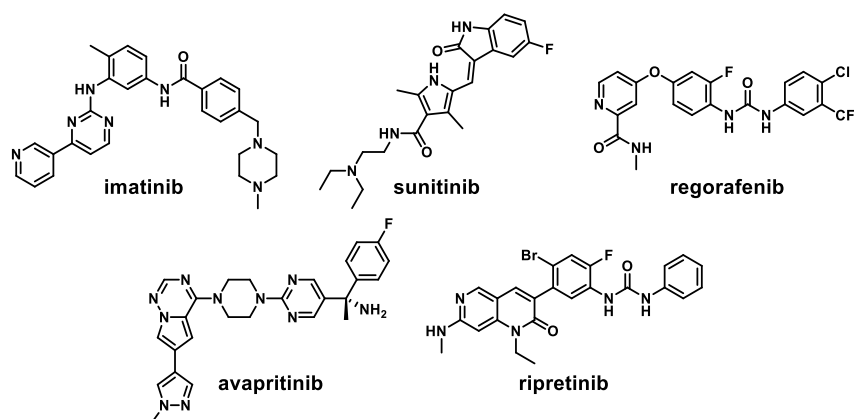

Figure 1. Representative c-KIT inhibitors.

In addition to clinically approved drugs, various scaffolds have been used as c-KIT inhibitors. A potent dual c-KIT/PDGFRα 1*H*-pyrazolo[3,4-*b*]pyridine inhibitor for the treatment of imatinib-resistant GISTs has been reported [28], but its anti-proliferative activity against TEL-c-KIT D816V Ba/F3 cells was not significant (GI$_{50}$ > 10 μM). The derivatives having the 2-aminothiazole scaffold switch off activated c-KIT to its inacti-vated state, and possess activities against constitutively activated mutants in the activation loop [29]. Moreover, the thiazolo[5,4-*b*]pyridine scaffold has been used to discover various

kinase inhibitors against PI3K [30], ITK [31], BCR-ABL [32], RAF [33], and VEGFR2 [34]. Thiazolo[5,4-*b*]pyridine derivatives have distinct types of binding modes depending on target kinases. The 4-nitrogen of thiazolo[5,4-*b*]pyridine is hinge-binding motif of PI3K kinase inhibitors while the 1-nitrogen and 2-amino group of the scaffold form H-bonding contact with the ITK kinase hinge region. In addition, the 5-position of thiazolo[5,4-*b*]pyridine has been functionalized to target the ATP-binding site of BCR-ABL, RAF, and VEGFR2. It is worthwhile to note that this study has, for the first time, reports functionalization on the 6-position of thiazolo[5,4-*b*]pyridine scaffold to identify novel c-KIT inhibitors.

In an effort to overcome drug resistance, we synthesized 31 novel thiazolo[5,4-*b*] pyridine derivatives and carried out a structure-activity relationship study against c-KIT enzyme and c-KIT-activated cells. The results of the SAR study for thiazolo[5,4-*b*]pyridine derivatives revealed that **6r** possesses higher enzymatic and anti-proliferative activities than imatinib and comparable activities relative to sunitinib. Notably, **6r** has 8.0-fold higher enzymatic inhibitory activity (IC_{50} = 4.77 μM) against c-KIT V560G/D816V double mutant and 23.6-fold higher anti-proliferative activity (GI_{50} = 1.15 μM) on HMC1.2 cells harboring both V560G and D816V c-KIT mutations compared with imatinib. Moreover, **6r** exhibits a reasonable selectivity in the biochemical kinase panel profiling. Furthermore, **6r** suppresses proliferation of cancer cells (GIST-T1 and HMC1.2) and c-KIT D816V Ba/F3 cells via blockade of c-KIT downstream signaling, and induction of apoptosis and cell cycle arrest. Notably, **6r** remarkably blocks migration and invasion, as well as anchorage-independent growth of GIST-T1 cells.

2. Materials and Methods

2.1. Chemistry

All commercial reagents and solvents were purchased from chemical suppliers and directly used for synthesis without purification. Reaction monitoring was performed by thin-layer chromatography (TLC) analysis using a UV lamp, ninhydrin, or *p*-anisaldehyde stain for the compound detection. Reaction products were purified by column chromatography on silica gel (230−400 mesh). Purities of all compounds were analyzed by Waters LC/MS system and shown to be over 95%. ^{1}H and ^{13}C NMR spectra were recorded either by a Bruker 300 MHz FT-NMR (300 MHz for ^{1}H, and 75 MHz for ^{13}C) or a 400 MHz FT-NMR (400 MHz for ^{1}H, and 100 MHz for ^{13}C) spectrometer. The synthetic procedures and chemical characterizations of all compounds are described in File S1.

2.2. Cell Culture and Reagent

GIST-T1 (Cosmobio, Tokyo, Japan, # PMC-GIST01C-COS) cells were cultured in DMEM (Welgene, # LM001-05) and HMC1.2 (Merck, Darmstadt, Germany, # SCC062) cells were cultured in IMDM (Welgene, # LM004-01). Parental Ba/F3 (DSMZ, Braunschweig, Germany, # ACC300) cells were cultured in RPMI (Welgene, # LM011-51) with 10 ng IL-3/mL (Enzo, # ALX-201-821). The culture media was supplemented with 10% fetal bovine serum and 1% penicillin/streptomycin solution. The cells were maintained in a humidified atmosphere containing 5% CO_2 at 37 °C.

2.3. In Vitro Kinase Assay

Biochemical kinase assays on c-KIT protein kinase were performed at Reaction Biology Corp. (San Diego, CA, USA). Compounds were tested with 10 μM ATP in a 10-dose IC_{50} mode with 3-fold serial dilution. The bioluminescent-based kinase assay was tested using an ADP-Glo assay kit. c-KIT (V560G/D816V) kinase was purchased from Promega (# VA7063). Compounds were tested with 10 μM ATP in a 10-dose IC_{50} mode with 3-fold serial dilution. The kinase assay followed the manufacturer's instruction. IC_{50} values were calculated by GraphPad prism 8.0 software (GraphPad Software, San Diego, CA, USA).

2.4. Cell Viability Assay

Cells (GIST-T1: 5.0×10^3; HMC1.2: 1×10^4) were seeded in 96-well plates. Each compound was treated in each well at 10 dose points of 3-fold serial dilution. After treatment with each compound for 72 h, CellTiter-Glo solution (Promega, # G7572) was added to each well. Anti-proliferation activity was measured the luminescence using a 96-well plate reader (EnVision 2013).

2.5. Molecular Docking Study

The X-ray co-crystal structure of c-KIT complexed with imatinib (PDB code: 1T46) was retrieved from the Protein Data Bank and loaded into Maestro software (Schrödinger Release 2020-4, New York, NY, USA). The Protein Preparation Wizard was executed for replenishment of missing residue, addition of hydrogens, and assignment of bond orders. Restrained energy minimization was applicated in the OPLS3e force field. Ligand **6r** was prepared using the LigPrep and the receptor c-KIT grid was generated considering the imatinib binding pocket. Ligand docking of **6r** on c-KIT was performed using GLIDE.

2.6. Kinase Panel Profiling

Kinase panel profiling was conducted by Reaction Biology Corp. (San Diego, CA, USA). A single dose (1.0 μM) of **6r** was tested against 371 recombinant human kinases in the presence of 10 μM ATP.

2.7. Western Blot Analysis

Cells were harvested and lysed using RIPA buffer containing 50 mM HEPES (pH 7.4), 1% Triton X-100, 2 mM EDTA, 150 mM NaCl, 2.5 mM NaF, 5 mM Na_3VO_4, and protease inhibitor cocktail tablet (Roche, # 11–878-580–001). Proteins were separated and transferred to an NC membrane. The membranes were blocked using 5% skim milk in TBS-T buffer. The p-c-KIT (Tyr703, # 3073), p-AKT (Ser473, # 9271), p-ERK (Thr202/Tyr204, # 8544), ERK (# 4695), p-PLCγ (Tyr783, # 14008), p-STAT3 (Tyr705, # 4074), and PARP (# 9542) antibodies were obtained from Cell Signaling Technologies. The β-actin (# sc-47778) and STAT3 (# sc-482) antibodies were obtained from Santa Cruz Biotechnology. AKT (A18120) antibody was purchased from ABclonal. Each primary antibody was incubated overnight at 4 °C. The secondary antibody (GenDEPOT) was incubated for 1 h at room temperature. Proteins were detected using ECL substrate.

2.8. Cell Cycle Arrest and Apoptosis Analysis

After compound treatment in GIST-T1 and HMC1.2 cells for 24 h, cells were fixed with 70% cold ethanol. Then, cells were incubated with 50 μg propidium iodide/mL solution (PI, Sigma) containing 1 mg RNase A/mL for 30 min in the dark. Cell cycle arrest was analyzed (BD Accuri), and data were processed using BD Accuri™ C6 software. For apoptosis analysis, compound treatment for 24–48 h, cells were harvested and stained with annexinV and PI solution. 1×10^5 cells were analyzed using flow cytometric analysis.

2.9. Migration Assay

GIST-T1 cells were seeded in 6-well plates at 2×10^6 cells. Next day, cells were washed with PBS and wounded in the center of each well. Then, GIST-T1 cells were washed with PBS and added to fresh DMEM. After 36 h, the scratch recovery of GIST-T1 cells in each compound-treated groups were observed and taken with a Nikon microscope at a magnification of 1000×.

2.10. Invasion Assay

The cell invasion assay was performed using Transwell membrane filter inserts (Corning Costar Corp., Corning, NY, USA). GIST-T1 cells were then suspended in serum-free DMEM at 2×10^6 cells and seeded in the upper chambers. In the lower chambers, the

DMEM medium containing 10% FBS was added. After 48 h, the cells migrating down the membrane were stained with crystal violet.

2.11. Soft Agar Assay

Anchorage-independent growth was assessed by determining colony formation on soft agar. GIST-T1 cells in DMEM media containing 0.7% agar were plated at 5,000 cells per well. Cells were treated with each compound for 3 weeks, and the media were changed every 3 days. Colonies were stained using iodonitrotetrazolium chloride (Sigma Aldrich). The average number colonies were counted using ImageJ software (version 1.53e, National Institutes of Health, Bethesda, MD, USA)

2.12. Statistical Analysis

Statistical analysis was performed using GraphPad Prism 8.0. Graphpad software, San Diego, CA, USA. All data are reported as average $\pm$ standard deviation (S.D.). $p < 0.05$ was considered to be statistically significant.

3. Results and Discussion

3.1. Synthesis of Thiazolo[5,4-b]pyridine Derivatives

The synthetic route for the thiazolo[5,4-*b*]pyridine derivatives is described in Scheme 1. To synthesize thiazolo[5,4-*b*]pyridine scaffold, we carried out the aminothiazole formation using commercially available 3-amino-5-bromo-2-chloropyridine **1** and potassium thiocyanate in 75% yield. The amino group of **2** underwent Boc protection to afford compound **3** in 90% yield. Then, **3** was coupled with 2-methyl-5-nitrophenylboronic acid pinacol ester by Suzuki cross-coupling reaction using Pd(dppf)Cl$_2$ as catalyst to form **4** in 70% yield. Reduction of the nitro group of **4** afforded the key intermediate **5** in 80% yield. The amide formation of aniline **5** with various carboxylic acids, followed by subsequent Boc deprotection yielded **6a–i** and **6k–w**. Urea formation between aniline **5** and 3-(trifluoromethyl)phenyl isocyanate was followed by subsequent Boc deprotection gave **6j**. The primary amino group of selected derivatives was transformed into the corresponding amides **7a–h** in 21–38% yields.
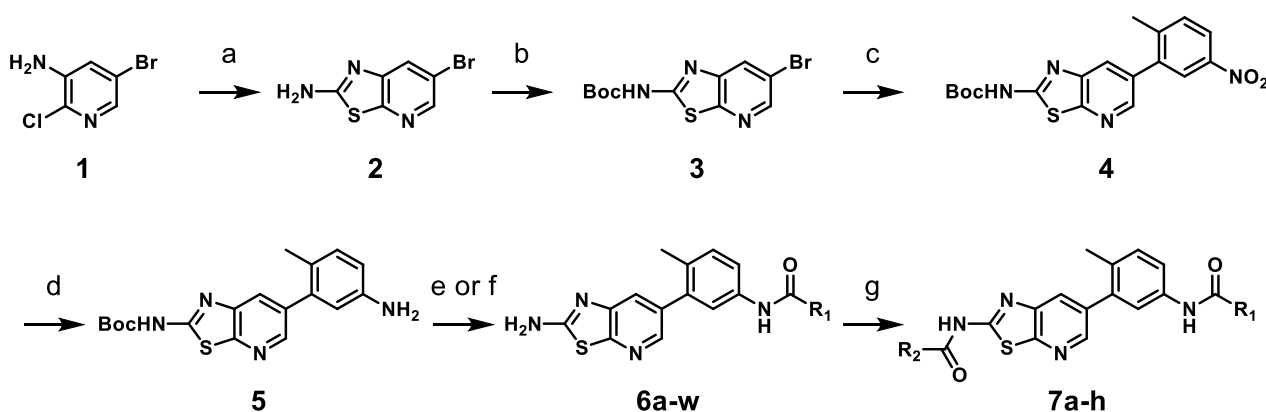
Scheme 1. Synthesis of thiazolo[5,4-*b*]pyridine derivatives **6a–w** and **7a–h**[a]. [a] Reagent and condition: (**a**) potassium thiocyanate, HCl, 100 °C, 12 h, 75%; (**b**) di-*tert*-butyl dicarbonate, DMAP, THF, rt, 90%; (**c**) 2-methyl-5-nitrophenylboronic acid pinacol ester, Pd(dppf)Cl$_2$, Na$_2$CO$_3$, DME/H$_2$O, 100 °C, 3 h, 70%; (**d**) iron powder, NH$_4$Cl, THF/MeOH/H$_2$O, 70 °C, 1 h, 80%; (**e**) (i) R$_1$-COOH, HATU, DIPEA, DMF, rt, 6 h; (ii) TFA, CH$_2$Cl$_2$, rt, 6 h, 21–65% (over 2 steps); (**f**) (i) 3-(trifluoromethyl)phenyl isocyanate, TEA, THF, rt; (ii) TFA, CH$_2$Cl$_2$, rt, 6 h, 53% (over 2 steps); (**g**) R$_2$-COCl, pyridine, CH$_2$Cl$_2$, rt, 3 h, 21–38%.
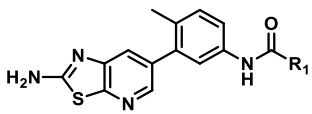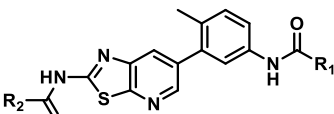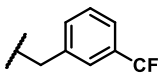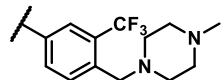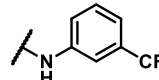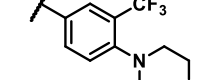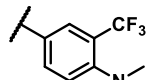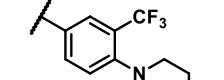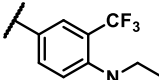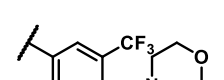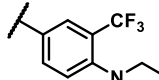
3.2. Structure-Activity Relationships

Enzymatic inhibitory activities of all synthesized thiazolo[5,4-*b*]pyridine derivatives against c-KIT were measured using radiometric biochemical kinase assays (Table 1). We first explored the R_1 group of the thiazolo[5,4-*b*]pyridine scaffold. The results show that only a 3-(trifluoromethyl)phenyl group (**6h**) resulted in a moderate enzymatic inhibitory activity (IC_{50} = 9.87 μM) among **6a–j** possessing five-membered and six-membered aromatic rings. Molecular docking study revealed that the 3-trifluoromethyl group fits well into the hydrophobic binding pocket [35]. Insertion of methylene group (**6i**) between the amide and 3-(trifluoromethyl)phenyl group of **6h,** and replacement of the amide with urea linkage (**6j**), as influenced by regorafenib and ripretinib, caused loss of enzymatic inhibitory activities.
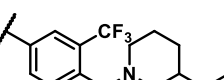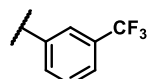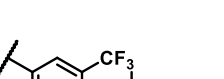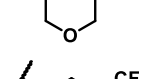
Table 1. Enzymatic inhibitory activities of thiazolo[5,4-*b*]pyridine derivatives **6a–w** and **7a–h** against c-KIT.

6a-w **7a-h**

Entry	R_1	R_2	IC_{50} (μM) [a]	Entry	R_1	R_2	IC_{50} (μM) [a]
imatinib	-	-	0.27	**6p**		-	5.72
sunitinib	-	-	0.14	**6q**		-	3.23
6a		-	inactive[b]	**6r**		-	0.14
6b		-	inactive[b]	**6s**		-	0.37
6c		-	inactive[b]	**6t**		-	1.25
6d		-	inactive[b]	**6u**		-	4.56
6e		-	inactive[b]	**6v**		-	0.39
6f		-	inactive[b]	**6w**		-	0.25
6g		-	inactive[b]	**7a**		cyclohexyl	1.51
6h		-	9.87	**7b**		phenyl	0.74

Table 1. *Cont.*

6a-w   **7a-h**

Entry	R_1	R_2	IC$_{50}$ (μM) ^{a}	Entry	R_1	R_2	IC$_{50}$ (μM) ^{a}
6i		-	inactive^b	7c		methyl	0.10
6j		-	inactive^b	7d		cyclohexyl	inactive^b
6k		-	4.31	7e		methyl	0.88
6l		-	1.76	7f		methyl	3.63
6m		-	2.17	7g		methyl	0.18
6n		-	Inactive ^{b}	7h		methyl	0.10
6o		-	5.03				

^{a} Radiometric biochemical kinase assay results. ^{b} less than 50% inhibition at a concentration of 10 μM.

To explore the effects of an additional substituent [36] on the 3-(trifluoromethyl)phenyl group of **6h**, we synthesized **6k–o** and evaluated enzymatic inhibitory activities. The results reveal that addition of 4-dimethylamino (**6k**), 4-morpholino (**6l**), and 4-methylpiperazino (**6m**) moiety on the *para*-position of the 3-(trifluoromethyl)phenyl group resulted in 2.3- to 5.6-fold enhanced activities (**6k**, IC$_{50}$ = 4.31 μM; **6l**, IC$_{50}$ = 1.76 μM; **6m**, IC$_{50}$ = 2.17 μM) compared with **6h**. In contrast, 3-morpholino (**6n**) and 4-methylpiperazino (**6o**) on the *meta*-position of 3-(trifluoromethyl)phenyl group brought about lower enzymatic inhibitory activities (**6n**, IC$_{50}$ = inactive; **6o**, IC$_{50}$ = 5.03 μM) relative to **6l** and **6m**. Therefore, *para*-substitution led to higher activities than *meta*-substitution.

Further investigation of *para*-substituents of the 3-(trifluoromethyl)phenyl group revealed that 4-morpholinomethyl group (**6p**) and (1,1-dioxidothiomorpholino)methyl group (**6q**) caused lower activities relative to 4-morpholino group (**6l**). Gratifyingly, **6r** having 4-((4-methylpiperazin-1-yl)methyl)-3-(trifluoromethyl)phenyl group possessed 15.5-fold

enhanced activity (IC_{50} = 0.14 μM) compared to **6m** (IC_{50} = 2.17 μM). The enzymatic inhibitory activity of **6r** was comparable to that of sunitinib (IC_{50} = 0.14 μM) and 1.9-fold higher than that of imatinib (IC_{50} = 0.27 μM). Encouraged by the promising enzymatic inhibitory activity of **6r**, further exploration of the 4-methylpiperazine group on **6r** was conducted. Removal of the 4-methyl group (**6s**) resulted in similar enzymatic inhibitory activity (IC_{50} = 0.37 μM) but substitution of the 4-methyl group with 2-hydroxyethyl group (**6t**) and acetyl group (**6u**) led to decreased activities. The derivatives with 4-(3-(dimethylamino)piperidin-1-yl)methyl group (**6v**) and 4-((2-(dimethylamino)ethyl)(methyl)amino)methyl group (**6w**) were less active than **6r**. On the basis of these results, the tail group of **6r** was selected and the R_2 group was further optimized.

Next, we focused on SAR study for the R_2 group. The effects of R_2 groups were explored by replacing the primary amino group on **6r** with the amide groups (**7a–c**). The results show that derivatives possessing cyclohexyl amide (**7a**, IC_{50} = 1.51 μM) and benzamide (**7b**, IC_{50} = 0.74 μM) had 5.3- to 10.8-fold decreased activities relative to **6r** (IC_{50} = 0.14 μM). On the other hand, the activity of **7c** having the acetamide group (IC_{50} = 0.10 μM) was slightly higher than that of **6r**. Similarly, among the derivatives **6l**, **7d**, and **7e**, **7e** possessing the acetamide group had slightly improved activities (**6l**, IC_{50} = 1.76 μM; **7d**, IC_{50} = inactive; **7e**, IC_{50} = 0.88 μM). The additional derivatives having the acetamide group (**7f–h**) were more active compared with the derivatives possessing the 2-amino group (**6p**, **6v**, and **6w**).

We assessed anti-proliferative activities of thiazolo[5,4-*b*]pyridine derivatives on c-KIT dependent cancer cells such as GIST-T1 and HMC1.2 (Table 2). The GIST-T1 was strongly positive for c-KIT and CD34, indicating that GIST-T1 cells had the characteristics of GIST [37]. The HMC1.2 cells bearing both c-KIT V560G in intracellular juxta-membrane region and c-KIT D816V in the kinase catalytic region caused SCF-independent constitutive activation of c-KIT [38,39]. The anti-proliferative activities of **6r**, **6s**, **7c**, and **7h** on GIST-T1 cancer cells were comparable or slightly higher relative to that of imatinib (GI_{50} = 0.02 μM). On HMC1.2 cells, the activities of **6k**, **6o**, **6r**, **6s**, and **7c** were higher than that of sunitinib (GI_{50} = 2.53 μM). It is worth noting that **6r** possessed 23.6-fold higher anti-proliferative activity (GI_{50} = 1.15 μM) on HMC1.2 cells than imatinib (GI_{50} = 27.10 μM). The SAR results reveal that **6r**, **6s**, and **7c** were able to strongly suppress the proliferation of GIST-T1 and HMC1.2 cancer cells.

Table 2. Anti-proliferative activities of thiazolo[5,4-*b*]pyridine derivatives **6a–w** and **7a–h** against GIST-T1 and HMC1.2 cells.

Entry	GI_{50} (μM) [a]		Entry	GI_{50} (μM) [a]	
	GIST-T1	HMC1.2		GIST-T1	HMC1.2
imatinib	0.02 ± 0.01	27.10 ± 3.36	**6p**	0.66 ± 0.10	8.55 ± 2.40
sunitinib	0.01 ± 0.00	2.53 ± 0.35	**6q**	0.42 ± 0.07	15.53 ± 3.97
6a	> 50	Inactive [b]	**6r**	0.01 ± 0.00	1.15 ± 0.96
6b	33.05 ± 7.09	Inactive [b]	**6s**	0.02 ± 0.00	1.33 ± 0.43
6c	33.69 ± 3.45	Inactive [b]	**6t**	0.12 ± 0.03	6.62 ± 0.75
6d	16.36 ± 2.73	25.18 ± 2.21	**6u**	0.66 ± 0.08	11.31 ± 0.34
6e	3.45 ± 0.41	11.53 ± 0.62	**6v**	0.05 ± 0.01	6.81 ± 0.67
6f	20.94 ± 2.00	inactive [b]	**6w**	0.02 ± 0.01	4.99 ± 0.43
6g	10.84 ± 1.06	36.77 ± 10.9	**7a**	0.08 ± 0.01	4.58 ± 0.32
6h	0.96 ± 0.10	7.26 ± 4.13	**7b**	0.10 ± 0.01	5.22 ± 0.59
6i	7.16 ± 0.87	9.65 ± 1.06	**7c**	0.01 ± 0.00	1.52 ± 0.43
6j	3.31 ± 0.73	6.35 ± 0.32	**7d**	8.13 ± 1.81	inactive [b]
6k	0.18 ± 0.03	2.27 ± 0.84	**7e**	0.23 ± 0.07	14.04 ± 10.2
6l	0.08 ± 0.01	4.34 ± 1.31	**7f**	0.30 ± 0.06	28.39 ± 13.3
6m	0.27 ± 0.17	3.41 ± 1.49	**7g**	0.07 ± 0.01	4.88 ± 1.18
6n	0.55 ± 0.09	7.00 ± 2.68	**7h**	0.02 ± 0.00	4.98 ± 0.32
6o	0.28 ± 0.08	2.36 ± 0.58			

[a] GI_{50} means the concentration at which a compound causes half-maximal growth inhibition. [b] less than 50% inhibition at a concentration of 50 μM.

Next, we evaluated enzymatic inhibitory activities of **6r**, **6s**, and **7c** against the c-KIT V560G/D816V double mutant (Table 3) [19]. These derivatives displayed 4.9- to 8.0-fold enhanced potency compared to imatinib (IC_{50} = 37.93 μM) and possessed comparable activities to sunitinib (IC_{50} = 3.98 μM) against the c-KIT V560G/D816V double mutant. Moreover, anti-proliferative activities of the **6r**, **6s**, and **7c** on c-KIT D816V Ba/F3 cells were evaluated (Table 4). On c-KIT D816V Ba/F3 cells, **6r** (GI_{50} = 1.11 μM), **6s** (GI_{50} =1.06 μM), and **7c** (GI_{50} = 0.53 μM) had comparable activities to sunitinib (GI_{50} = 0.58 μM). It is worthwhile to note that **6r**, **6s**, and **7c** possessed higher differential cytotoxicity than sunitinib on c-KIT D816V Ba/F3 cells relative to parental Ba/F3 cells, which implies that **6r**, **6s**, and **7c** would be more selective c-KIT inhibitors relative to sunitinib. These efforts led to the identification of novel thiazolo[5,4-*b*]pyridine derivatives that possessed enhanced anti-proliferative activities on c-KIT D816V Ba/F3 cells.

Table 3. Enzymatic inhibitory activities of thiazolo[5,4-*b*]pyridine derivatives **6r**, **6s**, and **7c** against c-KIT V560G/D816V.

Entry	IC_{50} (μM) [a]
	c-KIT V560G/D816V
imatinib	37.93 ± 8.68
sunitinib	3.98 ± 1.18
6r	4.77 ± 0.38
6s	7.67 ± 2.64
7c	5.07 ± 0.71

[a] ADP-Glo kinase assay.

Table 4. Anti-proliferative activities of thiazolo[5,4-*b*]pyridine derivatives **6r**, **6s**, and **7c** against c-KIT D816V Ba/F3 cells and parental Ba/F3 cells.

Entry	Ba/F3 cells GI_{50} (μM) [a]	
	c-KIT D816V	Parental
imatinib	12.25 ± 2.06	17.00 ± 0.20
sunitinib	0.58 ± 0.29	2.72 ± 0.30
6r	1.11 ± 0.47	8.06 ± 0.57
6s	1.06 ± 0.15	10.54 ± 3.59
7c	0.53 ± 0.06	10.52 ± 3.44

[a] GI_{50} means the concentration at which a compound causes half-maximal growth inhibition.

3.3. Molecular Docking Studies of 6j, 6r, and 7c with c-KIT

To investigate the binding mode of thiazolo[5,4-*b*]pyridine derivatives on c-KIT, we performed molecular docking studies of **6j**, **6r** and **7c** using the X-ray co-crystal structure of c-KIT complexed with imatinib (Figure 2). For comparison, the binding mode of imatinib on c-KIT is presented in Figure 2C (PDB code: 1T46) [40]. The results shows that **6r** and **7c** form a pair of hydrogen bonding with a Cys673 backbone in the hinge region. In addition, **6r** and **7c** also makes hydrogen bonding with Glu640/Asp810 and Ile789/His790 backbone, and these hydrogen bondings are also observed in the co-crystal structure of imatinib and c-KIT. Moreover, the thiazolo[5,4-*b*]pyridine moiety of **6r** and **7c** participates in hydrophobic interactions with Leu799, Val603, Ala621, and Val654. Furthermore, the 3-trifluoromethyl group of **6r** and **7c** fits well into the hydrophobic binding pocket which is also occupied by ponatinib [35]. However, **6j** could not form a hydrogen bonding with Asp810 observed in imatinib and could not fit into the hydrophobic binding pocket occupied by ponatinib. The predicted binding model suggests that **6r** and **7c** possess inhibitory activity, and **6j** is inactive against c-KIT.
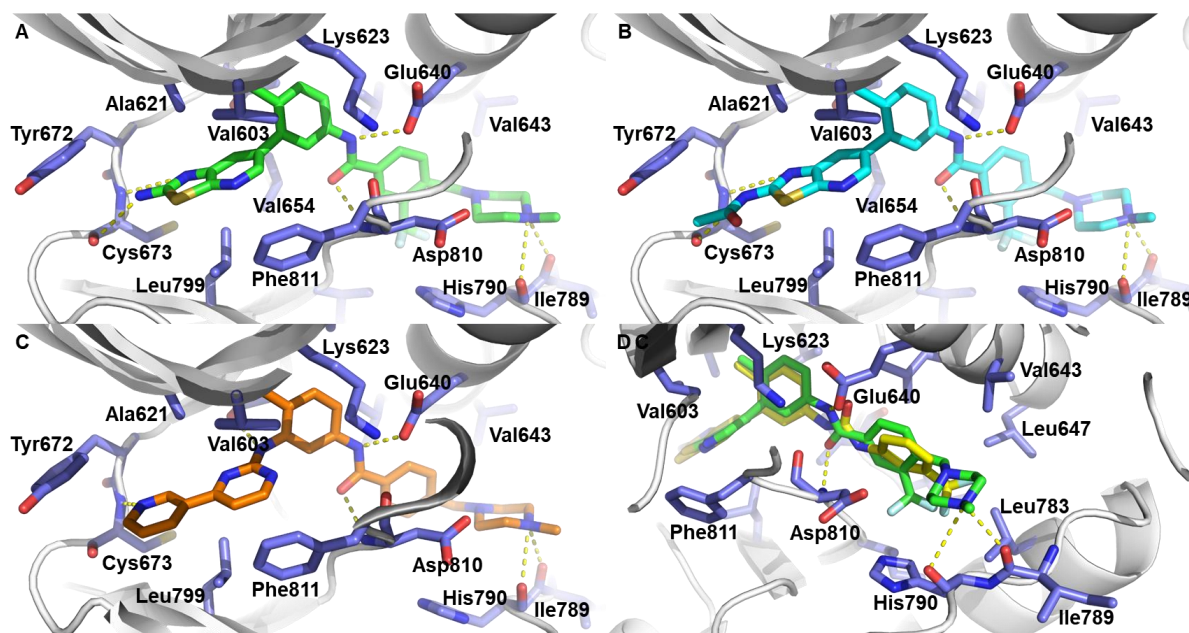
Figure 2. (**A**,**B**) Docking model prediction of **6r** and **7c** on c-KIT (PDB code: 1T46). (**C**) Binding mode of imatinib on c-KIT (PDB code: 1T46). (**D**) Superimposition with docking model of **6r** and **6j**. Protein residues of c-KIT are represented by white cartoon and violet stick. The **6j**, **6r**, **7c**, and imatinib are depicted in yellow, green, cyan, and orange, respectively.

3.4. Kinase Panel Profiling of 6r

Kinase panel profiling of **6r** showed that 13 of 371 kinases (c-KIT, RAF1, DDR1, RET, FMS, FRK, ARAF, LYN, BRAF, LCK, PDGFRa, P38a, PDGFRb) were inhibited more than 90% by **6r** (1 μM). The results reveal that **6r** possesses reasonable kinase selectivity (Figure 3 and Table S1).
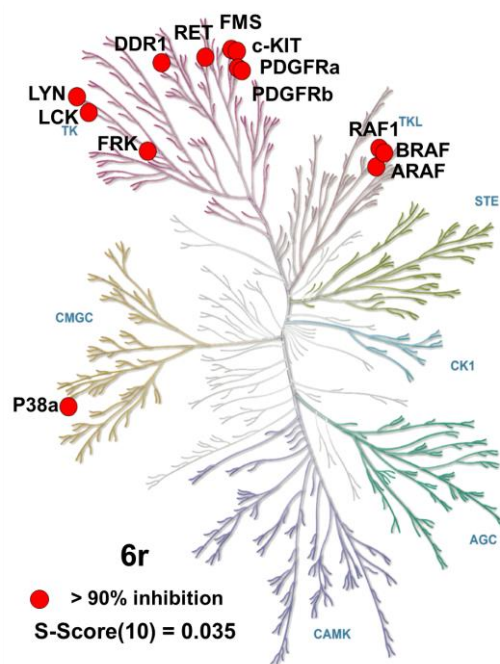

Figure 3. Kinase panel profiling of **6r**. Kinases that are more than 90% inhibited are represented by red circles. Illustration is provided by Cell Signaling Technology, Inc. (www.cellsignal.com, accessed on 3 November 2022) [41].

3.5. Inhibition of c-KIT Signaling in GIST-T1, HMC1.2, and c-KIT D816V Ba/F3 Cells

To assess that **6r**, **6s**, and **7c** are capable of inhibiting c-KIT auto-phosphorylation and suppressing downstream signaling, Western blot analysis was assessed using GIST-T1, HMC1.2, and c-KIT D816V Ba/F3 cells. Compound **6r**, **6s**, **7c**, and imatinib remarkably inhibited the levels of phosphorylated c-KIT (Tyr703) and its downstream signaling mediators including p-AKT, p-ERK, p-PLCγ and p-STAT3 in GIST-T1 cells (Figures 4A,B and S1A). On HMC1.2 and c-KIT D816V Ba/F3 cells, **6r**, **6s**, and **7c** at 10 μM concentration completely inhibited c-KIT auto-phosphorylation but not imatinib (Figures 4C–F and S1B,C). These results show that **6r**, **6s**, and **7c** blocked c-KIT downstream signaling associated with their anti-proliferation activities on GIST-T1, HMC1.2, and c-KIT D816V Ba/F3 cells.
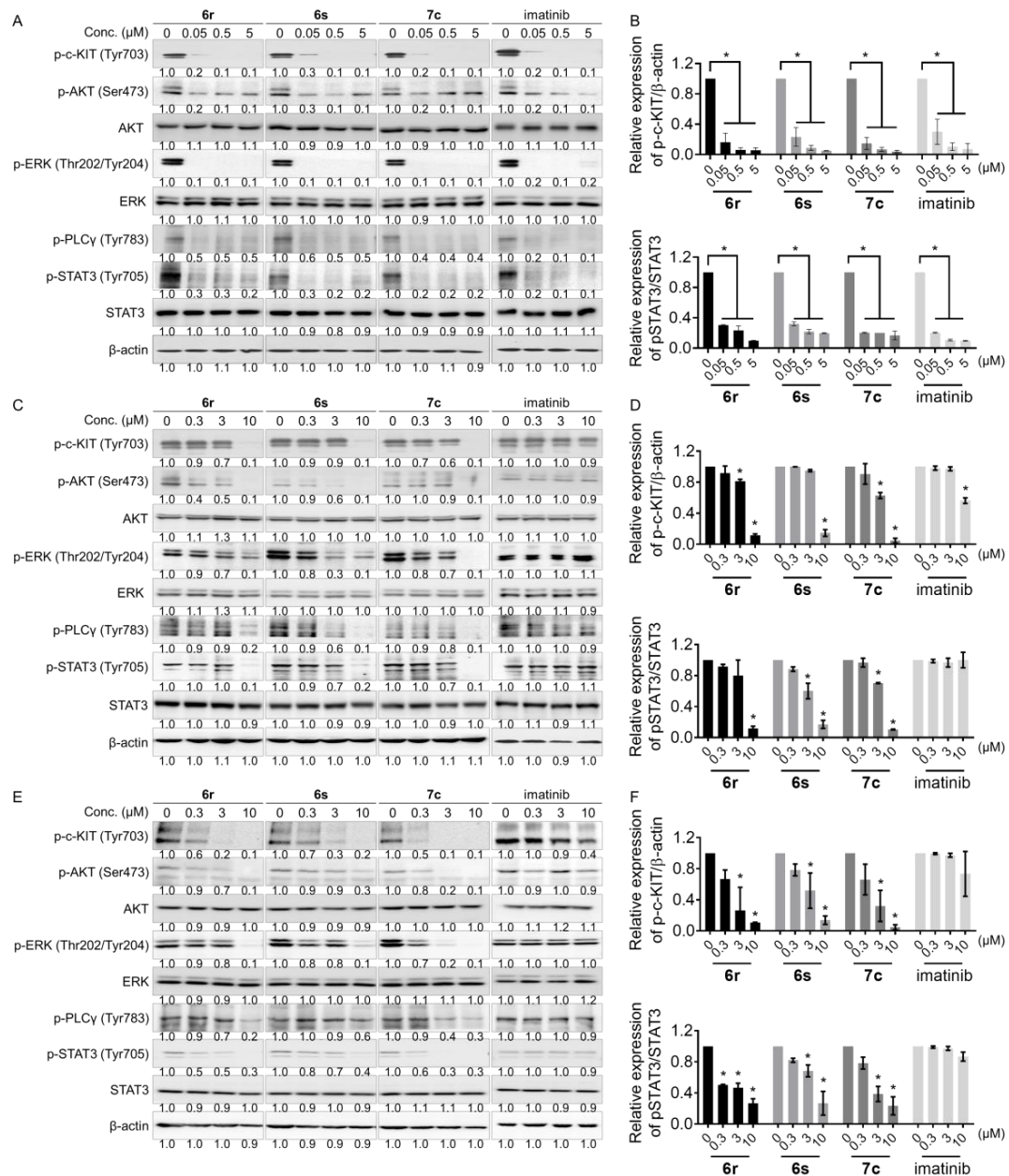

Figure 4. c-KIT and its downstream signaling are inhibited by **6r**, **6s**, and **7c** in (**A,B**) GIST-T1, (**C,D**) HMC1.2, and (**E,F**) c-KIT D816V Ba/F3 cells. Quantification of phosphorylated c-KIT and STAT3 levels by the treatment of **6r**, **6s**, and **7c** in GIST-T1, HMC1.2, and c-KIT D816V Ba/F3 cells. (average ± S.D., n = 3 one-way ANOVA; * $p < 0.05$).

3.6. Induction of Apoptosis and Cell Cycle Arrest in GIST- T1 and HMC1.2 Cells

Apoptosis and cell cycle arrest are important in cancer cell death [42,43]. PI3K/mTOR signaling by mutant c-KIT plays an important role in the tumor cell proliferation and apoptosis in GIST [44,45]. Moreover, c-KIT inhibitor induces apoptosis against mast cells [46]. The effects of **6r**, **6s**, and **7c** on apoptosis induction and cell cycle arrest were assessed in GIST-T1, HMC1.2, and c-KIT D816V Ba/F3 cells. As a result, **6r**, **6s**, and **7c** remarkably induced production of apoptotic cells in GIST-T1 (Figure 5A,B), HMC1.2 (Figure 5E,F), and c-KIT D816V Ba/F3 (Figure 5I,J) cells. It is worth noting that treatment with imatinib (1 µM) for 48 h did not induce apoptosis in HMC1.2 cells (Figure 5E,F). Moreover, induction of apoptosis by **6r**, **6s**, and **7c** was measured using apoptosis markers, which displayed that cleavage of PARP was induced in HMC1.2 cells (Figures 5M and S1D). We performed FACS analysis to determine whether **6r**, **6s**, **7c**, and imatinib induce cell cycle arrest in GIST-T1 and HMC1.2 cells. Treatment with **6r**, **6s**, **7c**, and imatinib (0.01 µM) induced G0/G1 arrest in 25–35% compared to control in GIST-T1 cells (Figure 5C,D). In addition, treatment with **6r**, **6s**, and **7c** (0.5 µM) for 24 h induced G0/G1 arrest more strongly in HMC1.2 and c-KIT D816V Ba/F3 cells compared with imatinib (Figure 5G,H,K,L). Collectively, these results indicate that **6r**, **6s**, and **7c** inhibit proliferation of GIST-T1, HMC1.2, and c-KIT D816V Ba/F3 cells through induction of apoptosis and cell cycle arrest.

3.7. Suppression of Migration and Invasion in GIST-T1 Cells

c-KIT is related to the migration and invasion of GIST cells [47]. To identify the effects of **6r**, **6s**, and **7c** on migration, we carried out a wound healing assay in the GIST-T1 cells (Figure 6A). Cell migration treated with **6r**, **6s**, **7c**, and imatinib (0.005 µM and 0.05 µM) was decreased by 50–70% compared to that of control (Figure 6C). Moreover, the migration ratio of GIST-T1 cells treated with **6r**, **6s**, **7c**, and imatinib deceased with increasing concentration. We conducted an invasion assay to further test the effects of **6r**, **6s**, and **7c** on invasion (Figure 6B) and found that **6r**, **6s**, and **7c** were capable of significantly suppressing the invasion capability of GIST-T1 cells (Figure 6D).
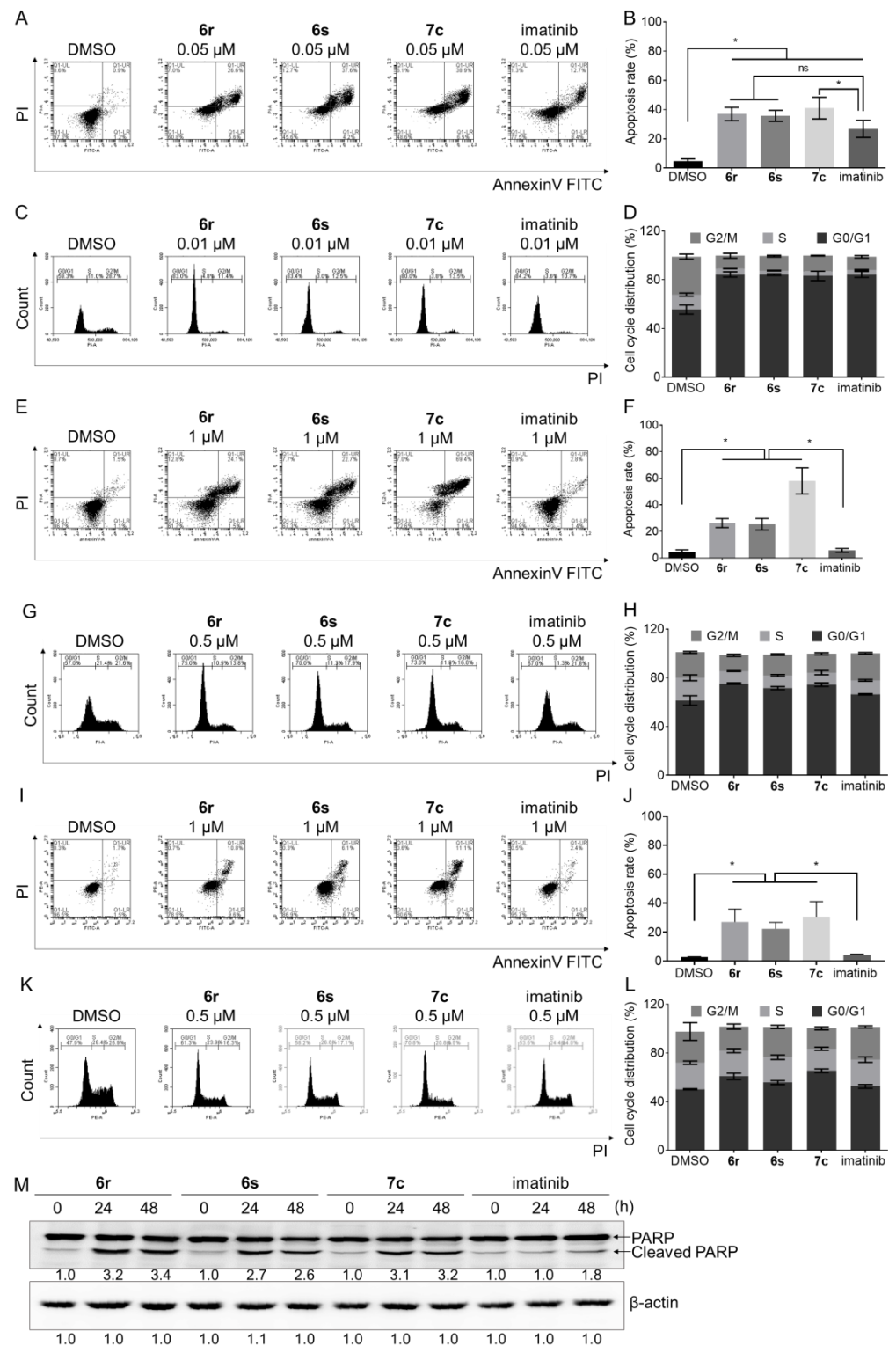
Figure 5. Effects of **6r**, **6s**, **7c**, and imatinib on induction of apoptosis and cell cycle arrest in (**A–D**) GIST-T1 (0.05 μM), (**E–H**) HMC1.2 (1 μM), and (**I–L**) c-KIT D816V Ba/F3 (1 μM) cells. Cells were stained AnnexinV-FITC and PI. Flow cytometry analysis was assessed to determine the percentage of apoptotic cell. Treatment (24 h) with **6r**, **6s**, **7c**, and imatinib induced G0/G1 arrest in GIST-T1 (0.01 μM), HMC1.2 (0.5 μM), and c-KIT D816V (0.5 μM) Ba/F3 cells. (**M**) Treatment (24 and 48 h) with **6r**, **6s**, **7c**, and imatinib induced PARP cleavage in HMC1.2 cells. (average $\pm$ S.D., n = 3 one-way ANOVA and Tukey's multiple comparisons test; * $p < 0.05$. ns: not significant).
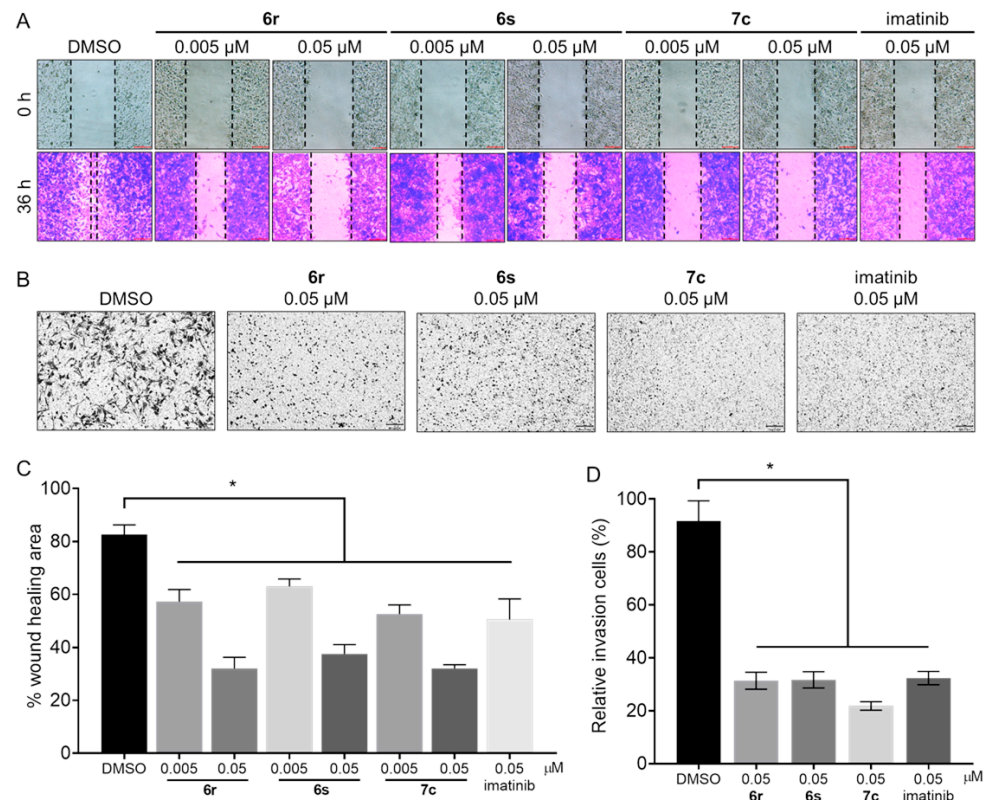
Figure 6. Effects of **6r**, **6s**, **7c**, and imatinib on migration and invasion. (**A**) Cell migration of GIST-T1 cells was inhibited by treatment (36 h) with **6r**, **6s**, and **7c** (0.005 μM and 0.05 μM). (**B**) Invasion of GIST-T1 cells was inhibited by treatment (48 h) with **6r**, **6s**, **7c**, and imatinib (0.05 μM). (**C,D**) Percentage wound healing area and relative invasion cells were calculated using ImageJ. (average ± S.D., n = 3 one-way ANOVA and Tukey's multiple comparisons test; * $p < 0.05$).

3.8. Suppression of Anchorage-Independent Growth in GIST-T1 Cells

Pharmacological inhibition and knockdown of c-kit decreased the colony growth of GIST cells [48]. A soft agar assay in GIST-T1 cells was performed to evaluate whether **6r** blocks anchorage-independent growth (Figure 7). Treatment with two different concentrations of **6r** and imatinib for 3 weeks resulted in dramatic inhibition of anchorage-independent growth of the GIST-T1 cells. Notably, incubation of **6r** at 0.05 μM completely suppressed anchorage-independent growth compared to control, indicating that blockade of c-KIT by **6r** suppresses tumorigenesis of GIST-T1 cells.
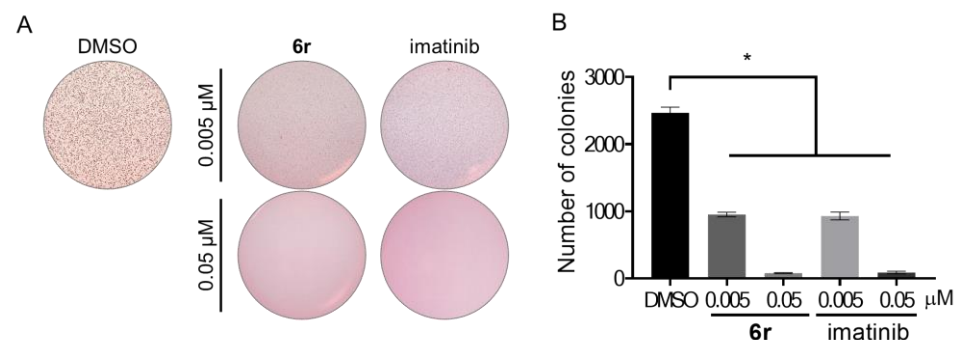

Figure 7. Effects of **6r** and imatinib on anchorage-independent growth. (**A**) GIST-T1 cells were cultured in 0.35% agar for 3 weeks. (**B**) The number of colonies was counted using ImageJ. (average ± S.D., n = 3 one-way ANOVA and Tukey's multiple comparisons test; * $p < 0.05$).

4. Conclusions

Dysregulation of c-KIT is associated with GIST. In order to identify a unique class of c-KIT inhibitors capable of inhibiting clinically relevant c-KIT mutations and overriding imatinib resistance, we designed and synthesized 31 novel thiazolo[5,4-*b*]pyridine derivatives and carried out structure-activity relationship studies against c-KIT enzyme and c-KIT activated cells. The results of SAR studies show that **6r**, **6s**, and **7c** possessed higher enzymatic and cellular activities than imatinib and these three derivatives were comparable to sunitinib in terms of activities. In particular, **6r** hand a 8.0-fold higher enzymatic inhibitory activity against c-KIT V560G/D816V double mutant and 23.6-fold higher anti-proliferative activity on HMC1.2 cells than imatinib, indicating that **6r** would be a promising lead for overriding imatinib resistance. It is of note that, compared with sunitinib, **6r** had a higher differential cytotoxicity effect on c-KIT D816V Ba/F3 cells relative to parental Ba/F3 cells, which suggests that **6r** is more selective c-KIT D816V inhibitor than sunitinib.

The analysis of molecular docking studies suggests that **6r** forms hydrogen bonding with a Cys673 backbone, Ile789/His790 backbone, and Glu640/Asp810. Moreover, the 3-trifluoromethyl group of **6r** occupies the hydrophobic binding pocket formed by Leu647, Ile653, Leu783, and Ile808. Kinase panel profiling showed that **6r** possesses a reasonable kinase selectivity and potent activities against 13 out of 371 kinases including c-KIT.

Western blot analysis revealed that **6r** significantly blocks c-KIT auto-phosphorylation and downstream signaling in GIST-T1, HMC1.2, and c-KIT D816V Ba/F3 cells. Compounds **6r**, **6s**, and **7c** induce more significantly apoptosis than imatinib on HMC1.2 cells. In addition, **6r**, **6s**, and **7c** are capable of blocking cell motility and suppressing anchorage-independent growth of GIST-T1 cells. Taken together, the novel thiazolo[5,4-*b*]pyridine derivatives provide insights into the design of novel c-KIT inhibitors capable of overcoming imatinib resistance.

Abbreviations

GIST, Gastrointestinal stromal tumor; PDGFR, Platelet-derived growth factor receptor; HMC, Human mast cell.

References

1. Broudy, V.C.; Lin, N.L.; Sabath, D.F. The fifth immunoglobulin-like domain of the Kit receptor is required for proteolytic cleavage from the cell surface. *Cytokine* **2001**, *15*, 188–195. [CrossRef] [PubMed]
2. de Silva, C.M.; Reid, R. Gastrointestinal stromal tumors (GIST): C-kit mutations, CD117 expression, differential diagnosis and targeted cancer therapy with Imatinib. *Pathol. Oncol. Res.* **2003**, *9*, 13–19. [CrossRef] [PubMed]

3. Pittoni, P.; Piconese, S.; Tripodo, C.; Colombo, M.P. Tumor-intrinsic and-extrinsic roles of c-Kit: Mast cells as the primary off-target of tyrosine kinase inhibitors. *Oncogene* **2011**, *30*, 757–769. [CrossRef]

4. Babaei, M.A.; Kamalidehghan, B.; Saleem, M.; Huri, H.Z.; Ahmadipour, F. Receptor tyrosine kinase (c-Kit) inhibitors: A potential therapeutic target in cancer cells. *Drug Des. Dev. Ther.* **2016**, *10*, 2443–2459. [CrossRef]

5. Ali, S.; Ali, S. Role of *c-kit*/SCF in cause and treatment of gastrointestinal stromal tumors (GIST). *Gene* **2007**, *401*, 38–45. [CrossRef] [PubMed]

6. Corless, C.L.; Fletcher, J.A.; Heinrich, M.C. Biology of gastrointestinal stromal tumors. *J. Clin. Oncol.* **2004**, *22*, 3813–3825. [CrossRef]

7. Steigen, S.E.; Eide, T.J. Gastrointestinal stromal tumors (GISTs): A review. *Apmis* **2009**, *117*, 73–86. [CrossRef]

8. Tabone-Eglinger, S.; Subra, F.; El Sayadi, H.; Alberti, L.; Tabone, E.; Michot, J.-P.; Théou-Anton, N.; Lemoine, A.; Blay, J.-Y.; Emile, J.-F. KIT mutations induce intracellular retention and activation of an immature form of the KIT protein in gastrointestinal stromal tumors. *Clin. Cancer Res.* **2008**, *14*, 2285–2294. [CrossRef]

9. Liang, J.; Wu, Y.-L.; Chen, B.-J.; Zhang, W.; Tanaka, Y.; Sugiyama, H. The C-Kit receptor-mediated signal transduction and tumor-related diseases. *Int. J. Biol. Sci.* **2013**, *9*, 435–443. [CrossRef]

10. Corless, C.L.; Barnett, C.M.; Heinrich, M.C. Gastrointestinal stromal tumours: Origin and molecular oncology. *Nat. Rev. Cancer* **2011**, *11*, 865–878. [CrossRef]

11. Antonescu, C.R.; Sommer, G.; Sarran, L.; Tschernyavsky, S.J.; Riedel, E.; Woodruff, J.M.; Robson, M.; Maki, R.; Brennan, M.F.; Ladanyi, M.; et al. Association of *KIT* exon 9 mutations with nongastric primary site and aggressive behavior: *KIT* mutation analysis and clinical correlates of 120 gastrointestinal stromal tumors. *Clin. Cancer Res.* **2003**, *9*, 3329–3337. [PubMed]

12. Vincenzi, B.; Napolitano, A.; Fiocco, M.; Mir, O.; Rutkowski, P.; Blay, J.-Y.; Reichardt, P.; Joensuu, H.; Fumagalli, E.; Gennatas, S.; et al. Adjuvant imatinib in patients with GIST harboring exon 9 KIT mutations: Results from a multi-institutional european retrospective study. *Clin. Cancer Res.* **2022**, *28*, 1672–1679. [CrossRef] [PubMed]

13. Napolitano, A.; Vincenzi, B. Secondary KIT mutations: The GIST of drug resistance and sensitivity. *Br. J. Cancer* **2019**, *120*, 577–578. [CrossRef] [PubMed]

14. Serrano, C.; Mariño-Enríquez, A.; Tao, D.L.; Ketzer, J.; Eilers, G.; Zhu, M.; Yu, C.; Mannan, A.M.; Rubin, B.P.; Demetri, G.D.; et al. Complementary activity of tyrosine kinase inhibitors against secondary kit mutations in imatinib-resistant gastrointestinal stromal tumours. *Br. J. Cancer* **2019**, *120*, 612–620. [CrossRef]

15. Zhang, J.Q.; Bosbach, B.; Loo, J.K.; Vitiello, G.A.; Zeng, S.; Seifert, A.M.; Medina, B.D.; Param, N.J.; Maltbaek, J.H.; Rossi, F.; et al. The V654A second-site KIT mutation increases tumor oncogenesis and STAT activation in a mouse model of gastrointestinal stromal tumor. *Oncogene* **2020**, *39*, 7153–7165. [CrossRef]

16. Li, B.; Wang, A.; Liu, J.; Qi, Z.; Liu, X.; Yu, K.; Wu, H.; Chen, C.; Hu, C.; Wang, W.; et al. Discovery of *N*-((1-(4-(3-(3-((6,7-dimethoxyquinolin-3-yl)oxy)phenyl)ureido)-2-(trifluoromethyl)phenyl)piperidin-4-yl)methyl)propionamide (CHMFL-KIT-8140) as a highly potent type II inhibitor capable of inhibiting the T670I "Gatekeeper" mutant of cKIT kinase. *J. Med. Chem.* **2016**, *59*, 8456–8472. [CrossRef]

17. Negri, T.; Pavan, G.M.; Virdis, E.; Greco, A.; Fermeglia, M.; Sandri, M.; Pricl, S.; Pierotti, M.A.; Pilotti, S.; Tamborini, E. T670X KIT mutations in gastrointestinal stromal tumors: Making sense of missense. *J. Natl. Cancer Inst.* **2009**, *101*, 194–204. [CrossRef]

18. Gajiwala, K.S.; Wu, J.C.; Christensen, J.; Deshmukh, G.D.; Diehl, W.; DiNitto, J.P.; English, J.M.; Greig, M.J.; He, Y.-A.; Jacques, S.L.; et al. KIT kinase mutants show unique mechanisms of drug resistance to imatinib and sunitinib in gastrointestinal stromal tumor patients. *Proc. Natl. Acad. Sci. USA* **2009**, *106*, 1542–1547. [CrossRef]

19. Ma, Y.; Zeng, S.; Metcalfe, D.D.; Akin, C.; Dimitrijevic, S.; Butterfield, J.H.; McMahon, G.; Longley, B.J. The c-*KIT* mutation causing human mastocytosis is resistant to STI571 and other KIT kinase inhibitors; kinases with enzymatic site mutations show different inhibitor sensitivity profiles than wild-type kinases and those with regulatory-type mutations. *Blood* **2002**, *99*, 1741–1744. [CrossRef]

20. Hochhaus, A.; La Rosée, P. Imatinib therapy in chronic myelogenous leukemia: Strategies to avoid and overcome resistance. *Leukemia* **2004**, *18*, 1321–1331. [CrossRef]

21. Lopes, L.F.; Bacchi, C.E. Imatinib treatment for gastrointestinal stromal tumour (GIST). *J. Cell Mol. Med.* **2010**, *14*, 42–50. [CrossRef] [PubMed]

22. Demetri, G.D.; Reichardt, P.; Kang, Y.-K.; Blay, J.-Y.; Rutkowski, P.; Gelderblom, H.; Hohenberger, P.; Leahy, M.; Von Mehren, M.; Joensuu, H.; et al. Efficacy and safety of regorafenib for advanced gastrointestinal stromal tumours after failure of imatinib and sunitinib (GRID): An international, multicentre, randomised, placebo-controlled, phase 3 trial. *Lancet* **2013**, *381*, 295–302. [CrossRef] [PubMed]

23. Yeh, C.-N.; Chen, M.-H.; Chen, Y.-Y.; Yang, C.-Y.; Yen, C.-C.; Tzen, C.-Y.; Chen, L.-T.; Chen, J.-S. A phase II trial of regorafenib in patients with metastatic and/or a unresectable gastrointestinal stromal tumor harboring secondary mutations of exon 17. *Oncotarget* **2017**, *8*, 44121–44130. [CrossRef]

24. Lübke, J.; Naumann, N.; Kluger, S.; Schwaab, J.; Metzgeroth, G.; Evans, E.; Gardino, A.K.; Lengauer, C.; Hofmann, W.-K.; Fabarius, A.; et al. Inhibitory effects of midostaurin and avapritinib on myeloid progenitors derived from patients with *KIT* D816V positive advanced systemic mastocytosis. *Leukemia* **2019**, *33*, 1195–1205. [CrossRef] [PubMed]

25. Grunewald, S.; Klug, L.R.; Mühlenberg, T.; Lategahn, J.; Falkenhorst, J.; Town, A.; Ehrt, C.; Wardelmann, E.; Hartmann, W.; Schildhaus, H.-U.; et al. Resistance to avapritinib in PDGFRA-driven GIST is caused by secondary mutations in the PDGFRA kinase domain. *Cancer Discov.* **2021**, *11*, 108–125. [CrossRef]

26. Smith, B.D.; Kaufman, M.D.; Lu, W.-P.; Gupta, A.; Leary, C.B.; Wise, S.C.; Rutkoski, T.J.; Ahn, Y.M.; Al-Ani, G.; Bulfer, S.L.; et al. Ripretinib (DCC-2618) is a switch control kinase inhibitor of a broad spectrum of oncogenic and drug-resistant KIT and PDGFRA variants. *Cancer cell* **2019**, *35*, 738–751. [CrossRef]

27. Serrano, C.; George, S. Gastrointestinal stromal tumor: Challenges and opportunities for a new decade. *Clin. Cancer Res.* **2020**, *26*, 5078–5085. [CrossRef]

28. Lu, Y.; Mao, F.; Li, X.; Zheng, X.; Wang, M.; Xu, Q.; Zhu, J.; Li, J. Discovery of potent, selective stem cell factor receptor/platelet derived growth factor receptor alpha (c-KIT/PDGFRα) dual inhibitor for the treatment of imatinib-resistant gastrointestinal stromal tumors (GISTs). *J. Med. Chem.* **2017**, *60*, 5099–5119. [CrossRef]

29. Wu, T.-S.; Lin, W.-H.; Tsai, H.-J.; Hsueh, C.-C.; Hsu, T.; Wang, P.-C.; Lin, H.-Y.; Peng, Y.-H.; Lu, C.-T.; Lee, L.-C.; et al. Discovery of conformational control inhibitors switching off the activated c-KIT and targeting a broad range of clinically relevant c-KIT mutants. *J. Med. Chem.* **2019**, *62*, 3940–3957. [CrossRef]

30. Xia, L.; Zhang, Y.; Zhang, J.; Lin, S.; Zhang, K.; Tian, H.; Dong, Y.; Xu, H. Identification of novel thiazolo [5,4-*b*]pyridine derivatives as potent phosphoinositide 3-kinase inhibitors. *Molecules* **2020**, *25*, 4630. [CrossRef]

31. Harling, J.D.; Deakin, A.M.; Campos, S.; Grimley, R.; Chaudry, L.; Nye, C.; Polyakova, O.; Bessant, C.M.; Barton, N.; Somers, D.; et al. Discovery of novel irreversible inhibitors of interleukin (IL)-2-inducible tyrosine kinase (Itk) by targeting cysteine 442 in the ATP pocket. *J. Biol. Chem.* **2013**, *288*, 28195–28206. [CrossRef] [PubMed]

32. Choi, H.G.; Zhang, J.; Weisberg, E.; Griffin, J.D.; Sim, T.; Gray, N.S. Development of 'DFG-out' inhibitors of gatekeeper mutant kinases. *Bioorg. Med. Chem. Lett.* **2012**, *22*, 5297–5302. [CrossRef] [PubMed]

33. Okaniwa, M.; Hirose, M.; Imada, T.; Ohashi, T.; Hayashi, Y.; Miyazaki, T.; Arita, T.; Yabuki, M.; Kakoi, K.; Kato, J.; et al. Design and synthesis of novel DFG-out RAF/vascular endothelial growth factor receptor 2 (VEGFR2) inhibitors. 1. exploration of [5,6]-fused bicyclic scaffolds. *J. Med. Chem.* **2012**, *55*, 3452–3478. [CrossRef]

34. Hirose, M.; Okaniwa, M.; Miyazaki, T.; Imada, T.; Ohashi, T.; Tanaka, Y.; Arita, T.; Yabuki, M.; Kawamoto, T.; Tsutsumi, S.; et al. Design and synthesis of novel DFG-out RAF/vascular endothelial growth factor receptor 2 (VEGFR2) inhibitors: 3. evaluation of 5-amino-linked thiazolo [5,4-*d*]pyrimidine and thiazolo [5,4-*b*]pyridine derivatives. *Bioorg. Med. Chem.* **2012**, *20*, 5600–5615. [CrossRef] [PubMed]

35. Garner, A.P.; Gozgit, J.M.; Anjum, R.; Vodala, S.; Schrock, A.; Zhou, T.; Serrano, C.; Eilers, G.; Zhu, M.; Ketzer, J.; et al. Ponatinib inhibits polyclonal drug-resistant KIT oncoproteins and shows therapeutic potential in heavily pretreated gastrointestinal stromal tumor (GIST) patients. *Clin. Cancer Res.* **2014**, *20*, 5745–5755. [CrossRef]

36. Cho, H.; Shin, I.; Ju, E.; Choi, S.; Hur, W.; Kim, H.; Hong, E.; Kim, N.D.; Choi, H.G.; Gray, N.S.; et al. First SAR study for overriding NRAS mutant driven acute myeloid leukemia. *J. Med. Chem.* **2018**, *61*, 8353–8373. [CrossRef]

37. Taguchi, T.; Sonobe, H.; Toyonaga, S.-I.; Yamasaki, I.; Shuin, T.; Takano, A.; Araki, K.; Akimaru, K.; Yuri, K. Conventional and molecular cytogenetic characterization of a new human cell line, GIST-T1, established from gastrointestinal stromal tumor. *Lab. Investig.* **2002**, *82*, 663–665. [CrossRef]

38. Sundström, M.; Vliagoftis, H.; Karlberg, P.; Butterfield, J.H.; Nilsson, K.; Metcalfe, D.D.; Nilsson, G. Functional and phenotypic studies of two variants of a human mast cell line with a distinct set of mutations in the c-kit proto-oncogene. *Immunology* **2003**, *108*, 89–97. [CrossRef]

39. Furitsu, T.; Tsujimura, T.; Tono, T.; Ikeda, H.; Kitayama, H.; Koshimizu, U.; Sugahara, H.; Butterfield, J.H.; Ashman, L.K.; Kanayama, Y. Identification of mutations in the coding sequence of the proto-oncogene c-kit in a human mast cell leukemia cell line causing ligand-independent activation of c-kit product. *J. Clin. Investig.* **1993**, *92*, 1736–1744. [CrossRef]

40. Mol, C.D.; Dougen, D.R.; Schneider, T.R.; Skene, R.J.; Kraus, M.L.; Scheibe, D.N.; Snell, G.P.; Zou, H.; Sang, B.-C.; Wilson, K.P. Structural basis for the autoinhibition and STI-571 inhibition of c-Kit tyrosine kinase. *J. Biol. Chem.* **2004**, *279*, 31655–31663. [CrossRef]

41. Eid, S.; Turk, S.; Volkamer, A.; Rippmann, F.; Fulle, S. KinMap: A web-based tool for interactive navigation through human kinome data. *BMC Bioinf.* **2017**, *18*, 1–6. [CrossRef] [PubMed]

42. Reyes-Sebastian, J.; Montiel-Cervantes, L.A.; Reyes-Maldonado, E.; Dominguez-Lopez, M.L.; Ortiz-Butron, R.; Castillo-Alvarez, A.; Lezama, R.A. Cell proliferation and inhibition of apoptosis are related to c-Kit activation in leukaemic lymphoblasts. *Hematology* **2018**, *23*, 486–495. [CrossRef] [PubMed]

43. Chang, F.; Steelman, L.S.; Shelton, J.G.; Lee, J.T.; Navolanic, P.M.; Blalock, W.L.; Franklin, R.; McCubrey, J.A. Regulation of cell cycle progression and apoptosis by the Ras/Raf/MEK/ERK pathway (Review). *Int. J. Oncol.* **2003**, *22*, 469–480. [CrossRef] [PubMed]

44. Bauer, S.; Duensing, A.; Demetri, G.D.; Fletcher, J.A. KIT oncogenic signaling mechanisms in imatinib-resistant gastrointestinal stromal tumor: PI3-kinase/AKT is a crucial survival pathway. *Oncogene* **2007**, *26*, 7560–7568. [CrossRef]

45. Bosbach, B.; Rossi, F.; Yozgat, Y.; Loo, J.; Zhang, J.Q.; Berrozpe, G.; Warpinski, K.; Ehlers, I.; Veach, D.; Kwok, A.; et al. Direct engagement of the PI3K pathway by mutant KIT dominates oncogenic signaling in gastrointestinal stromal tumor. *Proc. Natl. Acad. Sci. USA* **2017**, *114*, E8448–E8457. [CrossRef]

46. Juurikivi, A.; Sandler, C.; Lindstedt, K.A.; Kovanen, P.T.; Juutilainen, T.; Leskinen, M.J.; Mäki, T.; Eklund, K.K. Inhibition of c-kit tyrosine kinase by imatinib mesylate induces apoptosis in mast cells in rheumatoid synovia: A potential approach to the treatment of arthritis. *Ann. Rheum. Dis.* **2005**, *64*, 1126–1131. [CrossRef]

47. Zhou, Y.; Chen, J.; Weng, X.; Lin, G.; Huang, Z.; Shui, H. Establishment of a GIST-T1 gastrointestinal stromal tumour cell line resistant to imatinib mesylate. *Oncol. Lett.* **2018**, *15*, 7589–7594. [CrossRef] [PubMed]

48. Sun, J.; Zhang, Q.; Sun, X.; Xue, A.; Gao, X.; Shen, K. THZ1 targeting CDK7 suppresses c-KIT transcriptional activity in gastrointestinal stromal tumours. *Cell Commun. Signal.* **2022**, *20*, 138. [CrossRef]